doi:10.14311/ppt.2023.3.154
Plasma Physics and Technology **10**(3):154–158, 2023

OPTICAL INVESTIGATION OF A SPARK GAP FOR DC PROTECTION AROUND CURRENT ZERO

R. Methling[a,*], S. Schmausser[b], M. Kellermann[b], A. Ehrhardt[b], S. Gortschakow[a], D. Uhrlandt[a], D. Gonzalez[a]

[a] *Leibniz Institute for Plasma Science and Technology (INP), Felix-Hausdorff-Str. 2, 17489 Greifswald, Germany*

[b] *DEHN SE, Hans-Dehn-Str. 1, 92318 Neumarkt, Germany*

[*] methling@inp-greifswald.de

Abstract. The applied experimental setup consists of a pair of fixed electrodes forming a short gap in air. The electrodes are connected with a thyristor forming a parallel current path. Once the thought flashover ignited arc has burnt a given time in the range of several hundreds of microseconds, the thyristor will be fired causing a commutation of the current in the semiconductor path. Hence, the current through the electrode gap will be reduced. The extinguishment of the arc permits the creation of a current zero in the gap. The focus of the experimental work is set to the analysis of the arc plasma during the DC phase and its distinction in the current extinction phase (current zero). High speed camera observation and optical emission spectroscopy are carried out and combined with the electrical measurements.

Keywords: optical emission spectroscopy, DC protection, spark gap.

1. Introduction

The application of DC power grids has been continuously increasing for the last decades. With growing importance of renewable energies, electromobility, battery storage systems, and DC based electricity consumers like supercomputers, reliable DC switching and surge protection devices have been becoming essential. Surge protection devices based on spark gaps are widely investigated [1–5] and applied in low voltage AC systems [6, 7]. Basically, an arc is ignited after internal or externally induced high voltage surges, reducing thus the transient voltage and clearing the high surge current. Since the arc voltage is normally lower than that of the power supply, it has to be extinguished after surge clearance. In the AC case this is rather easily realized based on the natural zero crossing of the current, providing the transient recovery voltage is not high enough to reignite the arc after polarity change. However, in the DC case the absence of a natural current zero (CZ) makes it necessary not only to limit the arc current but also to force it to zero by external measures, avoiding thus a subsequent fault current.

An implementation of surge protection devices in DC systems can be realized by combination of mechanical and electronic switching based on power semiconductors. This principle of a hybrid surge protection device is already known for switches and spark gaps [8]. The fault current is commutated by the semiconductor, thus leading to arc extinction since the voltage drop of the semiconductor junction (some volts) is considerably lower than the required arc voltage (some tens of volts or more). Although this combination may provide a good functionality, it has two important disadvantages. First, the hard switching characteristic of the semiconductors, which shut the current flow off within very short times (ns to µs). In combination with the parasitic or normally used inductances in the grid, very high voltages can be eventually induced, leading to reignition of the gap or damaging devices. Second, to achieve feasible protection devices the used semiconductor has to be dimensioned to carry the fault current at least a minimum time until the dielectric strength of the spark gap is sufficiently recovered and capable to withstand the transient recovery voltage and/or the clamping voltage of in parallel connected varistors.

In this paper, we present first results of investigation on the radiating characteristics of post arc plasmas of a hybrid surge protection device for DC using spark gaps.

2. Experimental setup

An spark gap (SG) ignition circuit was used to initialize a discharge in the electrode gap. Within few microseconds, the discharge was transferred to a DC arc powered by a capacitor bank C1 of about 5.6 mF (400 V DC charge voltage via charging resistor R1). The current was limited by a serial resistor R2 to about 70 A. The arc voltage was about 30 V. In order to extinguish the DC arc, the electrodes were connected in parallel with a thyristor setup SCR, which could be triggered externally. After the desired arc operation time of either about 110 or 450 µs, the thyristor was be fired causing the current commutation and hence the extinguishment of the arc at the same time permitting to create a current zero in the electrode gap.

Electrode setup consists of two fixed, parallel copper

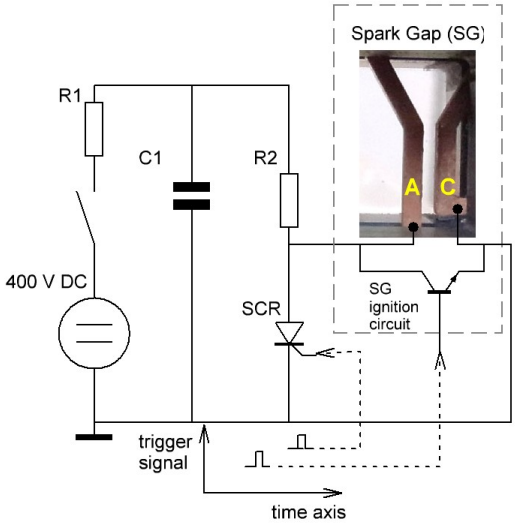

Figure 1. Electrical circuit and photograph of the electrode setup. Optical emission spectroscopy was carried out in the middle of the 1.6 mm gap between the electrodes at the position between the labels "A" and "C".

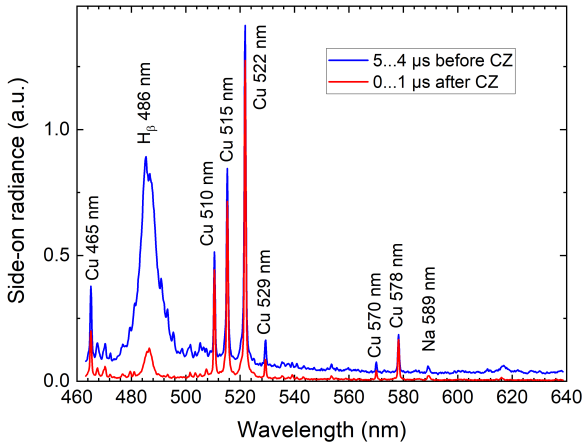

Figure 2. Spectrum: Atomic line emission can be assigned to the electrode material (Cu) and the surrounding gas (H_α 486 nm; other lines from hydrogen Balmer series, nitrogen and oxygen are not emitting in this spectral range).

λ (nm)	$g_u \times A_{ul}$ (10^8 s^{-1})	E_l (eV)	E_u (eV)
510.55	8.0E-02	1.389	3.817
515.32	2.4E+00	3.786	6.191
521.82	4.5E+00	3.817	6.192
522.01	6.0E-01	3.817	6.191

Table 1. Atomic data for selected Cu lines observed from discharge retrieved from NIST database.

rails with a width of about 4 mm (figure 1). The sharp, rectangular edge at the bottom of the right electrode (cathode) is the point of highest field strength and guarantees a stable ignition position. The electrodes are covered by windows made from either quartz or polycarbonate plates, forming a gap of 1.6 mm distance where the arc burns during most of the time and can be observed by optical methods.

Imaging was carried out using a high speed video camera (Photron Nova S6) equipped with metal interference filters. Optical emission spectroscopy (OES) along the electrode gap was applied at the position between the labels "A" and "C" in figure 1 using an imaging spectrograph (Roper Acton SpectraPro SP2500i) equipped with an ICCD camera (Princeton Instruments PI-MAX4). The spectra were dominated by atomic line emission that could be assigned either to the electrode material (Cu) and to the surrounding gas (see labels in figure 2). Beside nitrogen and oxygen atomic lines (mainly above 700 nm), also the Balmer series from hydrogen were found, mainly from remaining humidity in the air. Hints on wall ablation from polycarbonate windows was only found for high currents of 500 A and more (Swan bands from C_2 molecules). The spectrum acquired in the DC phase (blue curve in figure 2) has a higher intensity than the one taken immediately after current zero (red curve). It should be noted that the intensity decrease was strongest for the hydrogen line and less pronounced for the copper lines but not similar for all of them.

Selected properties of four atomic lines used for further analysis are listed in table 1. They were taken from the standard reference database provided by NIST [9]. Here, λ denotes the observed wavelength in air, $g_u \times A_{ul}$ the transition strength in units of $10^8\,s^{-1}$, and E_u and E_l the upper and the lower energy levels in eV, respectively. Since the two spectral lines at 522 nm originate from similar upper levels and were not spectrally resolved, they were combined as and treated as one line with summarized transition strength. Moreover, the 515 nm line has the same upper energy level and thus carries the same information on population densities. The 510 nm line, however, has a significantly lower energy level. The population of excited atomic states N is generally dependent on plasma temperature; the more hot the plasma, the higher atomic states become populated. Assuming local thermal equilibrium of the plasma, its temperature can be obtained by comparing relative line intensities originating from different upper energy levels by applying a Boltzmann plot. As a simplification of this standard method for temperature determination, in case of only two lines the ratio of line intensities can be applied. In the following, results will be shown for the 2-line method using the 522:510 nm ratio although it was proven that the 515:510 nm ratio delivered similar results.

3. Results and Discussion

The general behavior of the discharge was observed with high speed camera imaging. An upward movement along the rails with an average speed of about

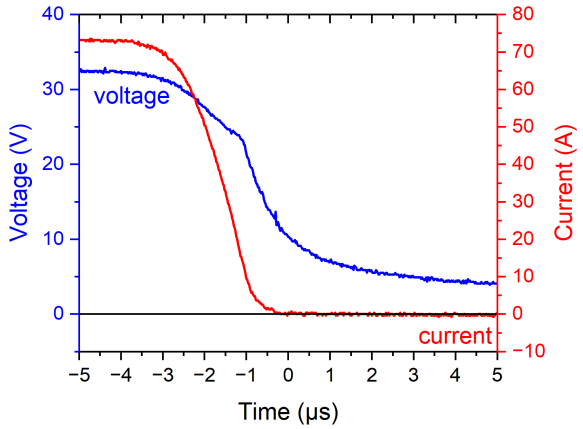

Figure 3. Electrical measurements during the current interruption period. DC arc current was switched off within 2-3 µs by short cut using a thyristor. Timescale was adjusted to current zero.

2 m/s was found. Using metal interference filters of different wavelengths the spatial distribution of the optical emission from the DC arc was investigated for different plasma components, e.g. copper, oxygen, hydrogen, or nitrogen. In case of atomic line emission of oxygen (O I 777 nm), a single cloud was observed in the middle between the electrodes with decreasing intensity towards the electrodes. In case of copper (Cu I 515 nm), the spatial distribution was quite different: Several small structures occurred near to the electrodes. The maximum intensity was close to the anode surface, like in the case of an anode spot or jet. Typically, a second, weaker spot appeared above and some hundred µs later became much brighter while the former spot disappeared, indicating a jumpwise change of the current connection at the anode side. It was concluded that the upward movement of the plasma was more a jumping than a smooth and continuous drift.

The focus for optical emission spectroscopy was set on the stable DC behavior (shortly before switch off) on the one side and the decay and cooling of the arc plasma after current interruption on the other side. Measurements of the electrical parameters around the time of current interruption are plotted in figure 3. The timeline was set according to termination of current flow through the electrode gap (current zero, red curve in figure 3). Since the decrease from the DC value of about 70 A to 0 A occurred within less than 4 µs, all time instants before -4 µs clearly belong to the DC arc phase. The fall time was determined to about 2.5 µs (90 % to 10 %). The arc voltage was about 30–34 V and its decrease was much slower (blue curve in figure 3) because of the thyristor used for the cut off that was connected in parallel electrode gap. Hence, around CZ mainly the thyristor voltage was measured that basically reflects the discharge voltage of the capacitor bank.

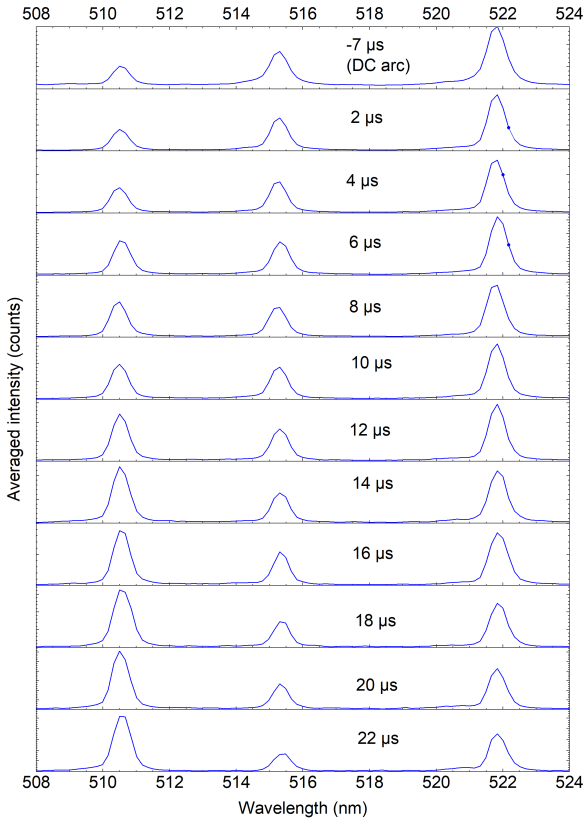

Figure 4. Details of optical emission spectra acquired at different time instants after current zero showing atomic lines of copper for 450 µs arc duration.

Using an intensified CCD camera just one optical emission spectrum could be acquired per shot. Series of optical emission spectra were taken with an exposure time of 1 µs and varying delays according to CZ (2-µs-steps). The exposure time was controlled using monitor pulses from the ICCD camera. For further analysis, the prominent atomic copper lines around 515 nm were applied. Hence, only the most interesting spectral range between 505 nm and 525 nm was plotted in figure 4. In the case of DC arc discharge the intensities of both the 522 nm and the 515 nm lines are considerably higher than that of the 510 nm line, indicating a temperature in the range of about 10 000 K or higher (cf. spectrum in the upper panel of figure 4). Within the following time after current interruption (and missing energy supply to the plasma), the overall intensities of all lines decrease by orders of magnitude. This showed that the density of the decaying plasma cloud was reduced. However, the decrease was faster for the lines at 515 nm and 522 nm than for the one at 510 nm. The sinking 522:510 nm line intensity ratio indicated a falling plasma temperature.

For a quantitative description, the plasma temperature was calculated with the 2-line method and plotted over time in relation to current zero in figure 5. In case of the arc duration of 450 µs as in the spectra of figure 4, a temperature of about 11 000 K was de-

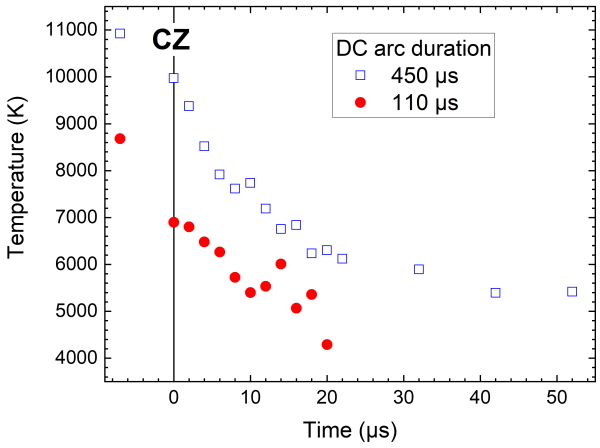

Figure 5. Plasma temperature in the DC arc phase before current zero and temperature decay in case of longer (blue) and shorter (red) arc duration.

termined for the DC arc, i.e. at a point of time 7 µs before current zero (blue open squares in figure 5). During the phase of current interruption, the temperature already decreased by about 700 K, resulting in a value around 10 000 K at CZ. In the following, a nearly exponential temperature decrease was found for the spectra shown in the lower panels of figure 5 reaching about 6 500 K at time instants around 20 µs. The absolute uncertainty of the temperature determination was estimated to less 1000 K, mainly based on the shot-to-shot reproducibility, the signal-to-noise ratio and a deviation of the relative sensitivity. The series were continued with 10 µs-steps. It was found that around 40–50 µs after CZ the temperature seemed to stabilize at values between 6 000 K and 5 000 K. However, during that phase the line intensities of 515 nm and 522 nm strongly decreased. Around 50 µs after CZ these lines with an upper energy level of 6.2 eV practically vanished into the background noise. Hence, increasing uncertainties of the line intensities and thus the calculated temperatures had to be regarded, making it practically impossible to determine reliable temperatures from a certain point of time. Still, the tendency derived from the spectra was clear since there were remaining intensities of the 510-nm line. In the investigated spectral range (460–640 nm), two other atomic copper lines exist with upper energy levels below 4 eV and sufficient transition strength, i.e. 570.02 nm (3.817 eV) and 578.21 nm (3.786 eV). These lines showed a very similar behavior to that of the 510-nm line. Moreover, the 578-nm line had a slightly slower intensity decrease than the two others until about 100 µs after current zero. That could be interpreted as a further hint for temperature decrease although the influence of decreasing copper density should be kept in mind.

The relevance of the duration of the DC arc before current termination was also investigated. Plasma temperatures before and after current zero for the case of 110 µs arc duration were plotted as filled red circles in figure 5. The temperature in the DC phase after about 110 µs was around 9 000 K, i.e. about 2 000 K less than for the longer discharges of about 450 µs. The decrease of the plasma temperature after current termination had a similar decay rate. Thus, temperatures around 5 000–6 000 K were reached already after 10–20 µs. That gives hints that smaller electrode gaps might be preferable for a fast decay of the hot plasma, maybe because of the cooling effect of the electrodes in case of low currents.

4. Summary and Conclusions

An experimental setup to investigate the intensity decay of the post arc plasma in a spark gap was successfully developed. The setup permits the study of the post arc radiation of DC arcs using high speed imaging and optical emission spectroscopy (OES). It was shown that even for a relatively low arc current (about 70 A DC) and few hundreds of microseconds, the plasma decay could be observed by the intensity of atomic copper lines for several 10 µs after current zero, with increasing uncertainty due to decrease of line intensities. Plasma temperatures in the post arc phase were calculated from line intensities of three copper lines at 510, 515 and 522 nm by application of the 2-line method. Temperatures around 11 000 K and 9 000 K in the case of the longer (450 µs) and shorter arc duration (110 µs) were obtained. After current commutation using a semiconductor and termination of the arc current in the electrode gap, an exponential temperature decay was observed. In case of longer arc duration a temperature close to the methodical limit of about 5 000–6 000 K was reached after 40–50 µs whereas for the shorter arc duration that point was reached considerably earlier (10–20 µs).

Generally, the intensity decrease depends on both the plasma temperature and the density. From OES not only the temperature of the post arc plasma could be obtained using the line intensity ratio but also some information about the decay of the plasma density could be assumed from the overall intensities. That gives hint on the post arc conductivity within the gap which is important for the dielectric recovery. It can be assumed that higher voltages should not be applied to the before at least 100 µs in case of the longer discharges and that discharge duration is a relevant parameter. Nevertheless, for a reliable estimation of the conductivity it would be necessary to determine the radiators density, too. Therefore, optical absorption spectroscopy (OAS) could be applied for the determination of metal vapor densities [10]. Another topic for the future will be an experimental determination of the dielectric recovery by means of electrical measurement of transient recovery voltage. Finally, the results obtained by optical (OES, OAS) and electrical methods should be compared.

Acknowledgements

This work has been funded by the German Federal Ministry for Economic Affairs and Climate Action (BMWK) within the framework of the AutoHybridS project, funding reference Nr. 03EI606. We would like to thank all the coworkers for their cooperation, support during experiments, and fruitful discussions that contributed to the progress of this work.

References

[1] L. Hüttner, L. Jurčacko, F. Valent, et al. Fundamental analysis of encapsulation of a low-voltage spark gap with deion chamber. In *Proc. of 19th Symposium on Physics of Switching Arcs*, pages 229–234, 2011.

[2] A. Ehrhardt, S. Schreiter, U. Strangfeld, and M. Rock. Encapsulated lighning current arrester with spark gap and deion chamber. In *Proc. of 19th Symposium on Physics of Switching Arcs*, pages 165–168, 2011.

[3] D. Bösche, M. Alija, M. Hilbert, and M. Kurrat. Investigation of the recovery behaviour of a small switching gap after current interruption. *Plasma Phys. Technol.*, 4:165–168, 2017. doi:10.14311/ppt.2017.2.165.

[4] T. Kopp, E. Peters, and M. Kurrat. Estimation of current density using high-speed-camera recordings in a model spark gap during surge currents. *Plasma Phys. Technol.*, 6:60–64, 2019. doi:10.14311/ppt.2019.1.60.

[5] G. Lo Piparo, R. Pomponi, T. Kisielewicz, et al. Protection against lightning overvoltages: Approach and tool for surge protective devices selection. *Electric Power Systems Research*, 188:106531, 2020. doi:10.1016/j.epsr.2020.106531.

[6] International Electrotechnical Commission. *IEC 62305, ed. 2.0, Protection against lightning. Parts 1-4*. IEC, Geneve, Switzerland, 2010-12.

[7] International Electrotechnical Commission. *IEC 60947-3, ed. 3.1, Low-voltage switchgear and controlgear. Part 3: Switches, disconnectors, switch-disconnectors and fuse-combination units*. IEC, Geneve, Switzerland, 2012-04.

[8] A. Ehrhardt and S. Schreiter. Dc arc extinguishing principles for spark gap. In *Proc. of 20th Symposium on Physics of Switching Arcs*, pages 131–134, 2013.

[9] A. Kramida, Y. Ralchenko, J. Reader, and NIST ASD Team. NIST atomic spectra database, version 5.9. URL: physics.nist.gov/asd.

[10] D. Hong, G. Sandolache, J. Bauchire, et al. A new optical technique for investigations of low-voltage circuit breakers. *IEEE Trans. Plasma Sci.*, 33:976–81, 2005. doi:10.1109/TPS.2005.844488.